



## Characterization and damage assessment of stones used in the Pasargadae World Heritage Site, Achaemenian period

Atefeh Shekofteh <sup>a</sup>, Eduardo Molina <sup>b,c</sup>, Anna Arizzi<sup>d</sup>, Giuseppe Cultrone<sup>d</sup>, Hossein Ahmadi<sup>a</sup>, and Mehdi Yazdi<sup>e</sup>

<sup>a</sup>Faculty of Conservation, Art University of Isfahan, Isfahan, Iran; <sup>b</sup>Department of Structural and Geotechnical Engineering, Pontificia Universidad Católica de Chile, Santiago, Chile; <sup>c</sup>Centro de Excelencia en Geotermia de los Andes (CEGA, FONDAP-CONICYT), Universidad de Chile, Santiago, Chile; <sup>d</sup>Faculty of Science, Department of Mineralogy and Petrology, University of Granada, Granada, Spain; <sup>e</sup>Faculty of Science, Geology Department, University of Isfahan, Isfahan, Iran

### ABSTRACT

The architectural remains at Pasargadae were built of three different stones classified according to their colors (beige, dark-gray, and green-gray). The stones show different macroscopic features, such as texture and decay patterns. The aim of this study is to identify the composition of the stones and to evaluate the main decay factors through petrographic studies in order to make conservation decisions more compatible. Petrochemical analyses show that the stones are in fact limestones with different features; two of them have a compact texture (beige and dark-gray stones), while the third has a fairly porous structure (green-gray stone). In some beige stone samples, dolomite was identified. Despite the fact that the presence of salt is a possible decay factor, X-ray diffraction analysis did not report any salt. According to SEM observations, the main reasons for decay in dark-gray and green-gray stones are the dissolution of calcite crystals and the swelling of clay minerals. The main decay factor in the beige stone, by contrast, is dissolution induced by microorganism activity. However, a patina formed by lichens on the surface of the beige stone, although aesthetically detrimental, protects it against further decay.

### ARTICLE HISTORY

Received 11 March 2017  
Revised 29 January 2018  
Accepted 31 January 2018

### KEYWORDS

biodeterioration; clay swelling; deterioration; dissolution; limestone; Pasargadae World Heritage Site

## 1. Introduction

A large number of the historical monuments and archaeological remains in Iran are made of stone, but very little research has so far been carried out to study their composition and the factors and mechanisms that cause them to decay. The Pasargadae World Heritage Site is one of the most important archaeological sites in Iran, as listed by UNESCO. It was the first dynastic capital of the Achaemenid Empire (559–330 BC), founded by Cyrus the Great (Stronach 1985) and is located 135 Km NE of Shiraz, in Fars province in southern Iran (Figure 1).

The archaeological site covers 1.6 square kilometers and consists of various different stone buildings. These include the remains of three palaces—the tomb of Cyrus the Great, the Zendān-e Soleyman tower, and the Toll-e Takht platform—and some isolated stone reliefs in the gateways to the palaces (Sami 1956; Tilia 1968). According to Tilia (1968), only two kinds of stone were used in the constructions at Pasargadae: a porous “yellow” sandstone and a dark-gray stone, which was harder and more compact than the yellowish stone, but not very

resistant. We found, however, that the building stones in Pasargadae can be divided into three main groups based on their color and appearance: beige stone, green-gray stone, and dark-gray stone. The beige stone was used in the construction of buildings, bases, and columns and the walls of the tomb of Cyrus and the Zendān-e Soleyman tower; the dark-gray stone was used as flooring for the palace, under the bases of the columns and in decorative features in the walls of the gateways; and the green-gray stone was used to build a rough platform on top of which the palaces themselves were built. This platform was covered with carved beige stones (Figure 1c).

The different stones at Pasargadae have decayed in different ways. The dark-gray stones used in the base of the columns have suffered more decay than the other two types. The stone blocks have layers with large cracks and in some cases the blocks have collapsed completely. In some cases, the green-gray stone blocks have also decayed resulting in granular disintegration (Figure 2). The beige stone seems to be in good condition, although some degree of biodeterioration is visible. The decay patterns

**CONTACT** Atefeh Shekofteh  [shekofte.as@gmail.com](mailto:shekofte.as@gmail.com)  Art University of Isfahan, Conservation of Historic and Cultural Artefacts, Hakim Nezami Street, Sangtarashha Lane, Isfahan, 1744, Iran.

Color versions of one or more of the figures in the article can be found online at [www.tandfonline.com/uarc](http://www.tandfonline.com/uarc).

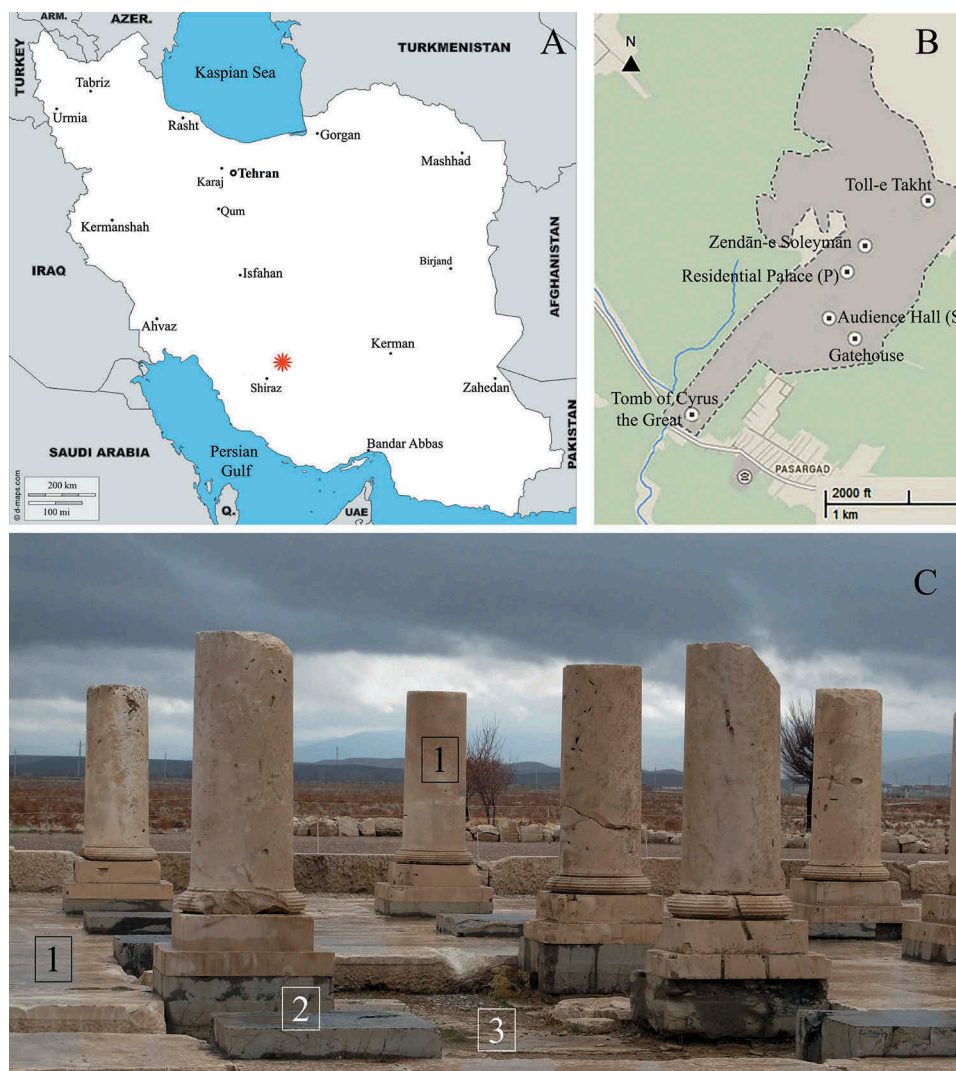


**Figure 1.** A) Map of Iran, the star marks the location of the Pasargadae site; B) Pasargadae World Heritage Site (from Google Map); C) Residential Palace where 1 is Beige stone, 2 is Dark-gray stone and 3 is Green-gray stone.

on Cyrus the Great's tomb were described by Rafiee Fanood and Saradj (2013).

The first step in the preservation of archaeological stone monuments is to characterize the stones and analyze their decay problems (Doehne Eric and Price 2010). Some conservation and restoration work has been conducted at Pasargadae. This involved joining broken fragments together and replacing damaged stones. The work was done in three phases: 1950s, 1970s, and 2006. During the initial restoration work in the 1950s, Portland cement was used to restore the damaged dark-gray stone and replace any missing pieces. In more recent work in 2006, polyester and epoxy stone adhesives were used to stick broken parts back together (Rafiee Fanood and Saradj 2013; Sami 1956). Two recent studies have characterized the types of fungi and lichens in Pasargadae. Ten different species of fungi (Mohammadi and Maghbolli-

Balasin 2014) and 20 species of lichens were identified (Haghighat 2014).

The conservation, maintenance, restoration, and substitution of stone artifacts require not only historical and artistic studies, but also proper knowledge of the materials that were used and in particular their chemical-mineralogical and textural properties. The state of alteration and decay must also be studied (Ashurst and Dimes 1998; Doehne Eric and Price 2010; Siegesmund, Weiss, and Vollbrecht 2002).

Decay in stones is generally caused by weathering processes (such as physical disintegration or chemical decomposition), which are highly dependent on the microstructural and mechanical characteristics of the stone as well as on environmental factors (Fitzner 2004; Moropoulou et al. 2003; Price 1995). This article focuses on the identification of the chemical composition and microstructure of the stone types used at the

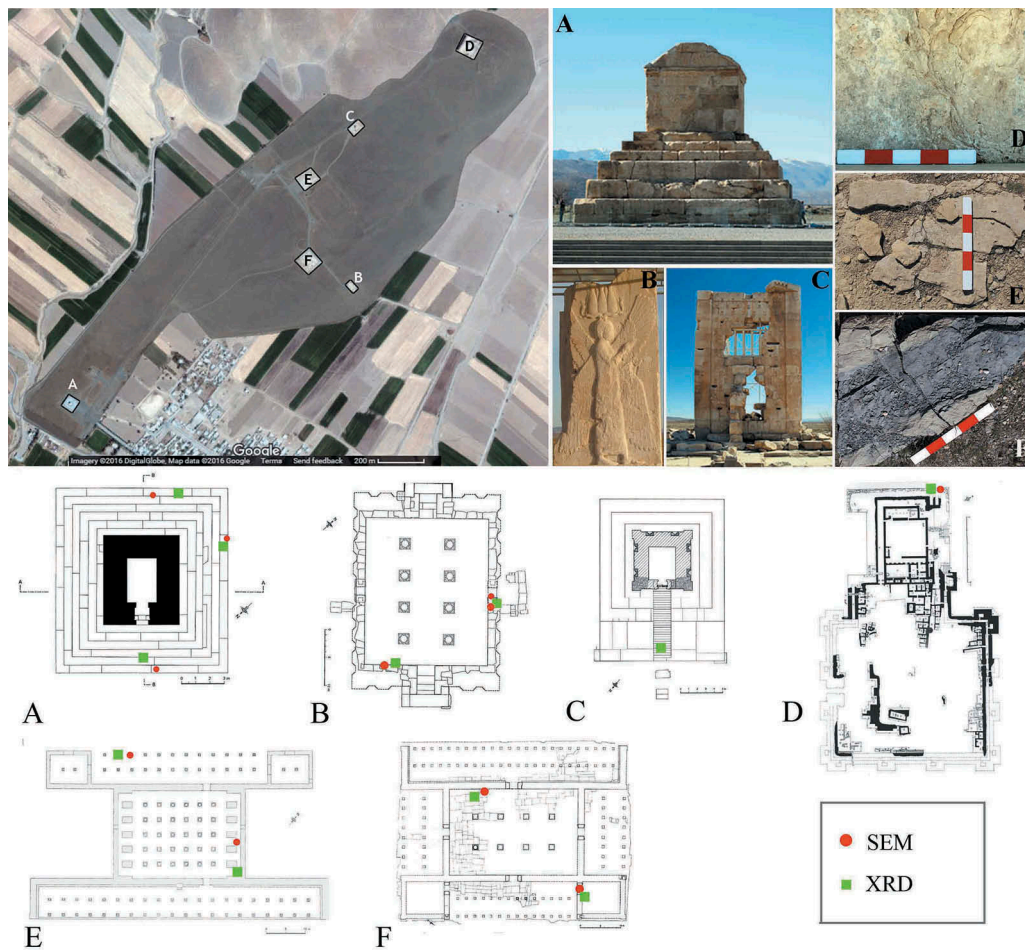


**Figure 2.** Top-left: bird's-eye view of the Pasargadae site showing the location of the monuments (from Google Earth); bottom: location of samples collected for SEM observation and location of the powder samples collected from damaged areas in order to identify probable salt phases by X ray diffraction analysis (maps source: Stronach, 1985). A) Tomb of Cyrus the Great; B) Winged Fig. inside Gatehouse; C) Zendān-e Soleymān; D) top: deterioration pattern (scaling) in beige stone from Toll-e Takht, bottom: location of samples; E) top: detachment and disintegration of green-gray stone from Residential Palace, bottom: location of resulting samples; F) top: collapsing upper part of dark-gray stone from Audience Hall.

Pasargadae World Heritage Site. We also study the patterns of decay on the surface of the stone and the most active decay factors. These studies were performed in order to be able to prepare an effective plan for the preservation of this important archeological site.

## 2. Materials and methods

Based on visual differences, three samples of beige stone (B1, B2, and B3), two samples of green-gray stone (GG1 and GG2) and two samples of dark-gray stone (DG1 and DG2) were collected from inner parts of some large fragments of broken stones, which can be found all over the Pasargadae site. All of these apparently undamaged, intact samples were subjected to mineralogical identification, petrographic observation, and chemical analysis.

In order to observe the influence of weathering at microscopic scale (e.g., presence of micro cracks, dehydration phenomena, etc.), small fragments were also collected from stone blocks in different buildings at the site (Table 1). All loose fragments, scaling, and peelings on the surface of the stone samples were removed. The samples collected for microscopic study are described in Table 1 and the location of each one is marked with a red circle in Figure 2.

Finally, in order to identify the possible presence of secondary phases that could explain the reasons for stone deterioration, we scraped powder samples from the same deteriorated parts of the monuments from which we had taken the weathered samples listed in Table 1. The location of these samples is shown in Figure 2 by green squares.

Powder X-ray diffraction (XRD) was performed in order to identify the mineralogy of the intact samples,

**Table 1.** Features of weathered samples collected at the site.

Sample Code	Stone type	Sampling Location	Description/Hypothesis of decay
B.C1	Beige	Cyrus Tomb, Northwest Side, First Stair	Peeling and scaling pattern/This side is in the shade almost all day and probably freezes during the winter
B.C2	Beige	Cyrus Tomb, Southeast Side, First Stair	Fragmentation/This side is exposed to sunlight for half of the day and the substrate may be subject to temperature fluctuation effects
B.C3	Beige	Cyrus Tomb, Southwest Side, First Stair	Pitting pattern/The surface of this sample is rough and has a pitting decay pattern probably due to microorganism activity
B.R1	Beige	Gatehouse, South side	Microorganism body/Lichen activity on the surface and pitting effects
B.R2	Beige	Relief of winged figure	Patina layer/Presence of a light-reddish patina
B.R3	Beige	Back of the relief of winged figure	Patina layer/Presence of a light-reddish patina and possible biodeterioration on the surface
B.T1	Beige	Toll-e Takht, Northwestern side	Patina layer/Almost all stone blocks in this monument are covered by orange patina, probably caused by lichen activity
GG.P1	Green-gray	Residential Palace, the lower floor	Moderate sanding problem/Probably due to differential hydric or thermal stress
GG.P2	Green-gray	Audience Hall, the lower floor	Microorganism on the surface/Pitting and biomineralization due to lichen activity
DG.S1	Dark-gray	Residential Palace, Southern side	Heavy delamination pattern/Physical separation into several layers may be due to the weakness of the texture or to freezing
DG.P1	Dark-gray	Audience Hall, Southern gate	Some microorganism activity on the surface and some delamination/Probably due to freezing

using a Philips PW-1710 diffractometer. Analysis conditions were: CuK $\alpha$  radiation ( $\lambda$ : 1.5405 Å), 3–60° 2 $\theta$  explored area, 45 kV voltage, and 40 mA current. The clay fraction obtained from the intact samples and the mineralogy of the deteriorated powders listed in Table 1 were analyzed using a Panalytical X'pert Pro MPD diffractometer with an automatic loader. Analysis conditions were as described above. The X-ray patterns were interpreted using X-Powder® software v.12 (Martín Ramos 2004). Quantitative analysis of the mineral phases was performed using the nonlinear least square method to fit full-profile diffractograms and the results were compared with standard values in the database. The PDF2 database and Normalized RIR method were used to identify the mineral phases. No internal standard mineral was added to the samples.

To determine the clay fraction, the samples were treated during several cycles with acetic acid (CH<sub>3</sub>COOH) in 1 N concentration in order to eliminate carbonates until no reaction process was observed. After washing, hydrogen peroxide (H<sub>2</sub>O<sub>2</sub>) at 20 vol.% was added to eliminate any possible organic matter. Samples were concentrated by removing the excess water and the fractions were separated below 2  $\mu$ m using a Kubota KS-8000 centrifuge. The concentrated fraction below 2  $\mu$ m was deposited on a glass sample-holder using the oriented aggregate method (OA). In order to determine the presence of swelling clays, oriented aggregates were solvated with ethylene-glycol (OA-EG) for 48 hr at 60°C (Bruton 1955). Samples were kept for 72 h at 80°C with dimethyl-

sulfoxide (OA-DMSO) to confirm the presence of kaolinite and were heated at 550°C for 90 min (OA-550) in order to destroy the kaolinite (if present) and to check for the presence of chlorite (González García and Sánchez Camazano 1968; Moore and Reynolds 1989).

The chemical composition of intact stones was determined using a Bruker S4 Pioneer X-ray fluorescence (XRF) spectrometer and the content was expressed as oxide weight (wt.%) normalized to 100% of the major and minor elements, LOI (Loss on ignition) was determined gravimetrically as the weight loss was recorded between 110°C and 1000°C.

The observation of the stone microstructure was carried out on thin sections on intact samples by means of polarized optical microscopy (POM), using a CarlZeiss Jenapol-U microscope equipped with a digital microphotography camera (Nikon D7000). A Leica videomicroscope model DVM2000 with a 50–400x lens (and a corrective lens of 0.4x) was used to perform surface observations on the weathered samples listed in Table 1, and the images were processed using the Leica Application Suite v3.8.0 (Leica Microsystems®).

The observation at microscale of the texture of samples was carried out using a BRUKER model Leo-Gemini field emission scanning electron microscope (FESEM) coupled with an energy dispersive spectrometer (EDX) on polished carbon-coated thin sections. The deteriorated parts and the patina collected from the monument were observed under high magnification by a TESCAN model MIRA III FESEM instrument, with a RONTEC backscattered electrons

**Table 2.** XRD data of the three types of stone.

B1		B2		B3		GG1		GG2		DG1		DG2	
Minerals	Amount (%)												
Calcite	100	Calcite	100	Calcite	47	Calcite	86	Calcite	88	Calcite	95	Calcite	97
				Dolomite	53	Quartz	14	Quartz	12	Quartz	5	Quartz	3

detector (BSE) and an energy dispersive spectrometer (EDX). All the samples were gold coated prior to the study.

### 3. Results

#### 3.1 Mineralogical and chemical study

XRD results presented in Table 2 confirm that all the stones are rich in carbonates. The beige stone is composed exclusively of calcite in B1 and B2, while sample B3 has similar amounts of calcite and dolomite. XRD analysis of the

green-gray stone (GG1 and GG2 samples) shows that the main phase is again calcite (about 85–90%). Quartz was detected as a minor phase. The major phase in the dark-gray stone (DG1 and DG2) is calcite (about 95%) with small amounts of quartz.

The clay fraction is composed of illite and small amounts of chlorite in the beige stone; illite, chlorite, and smectite in the green-gray stone; kaolinite and mixed layers of illite and chlorite in the dark-gray stone (Figure 3).

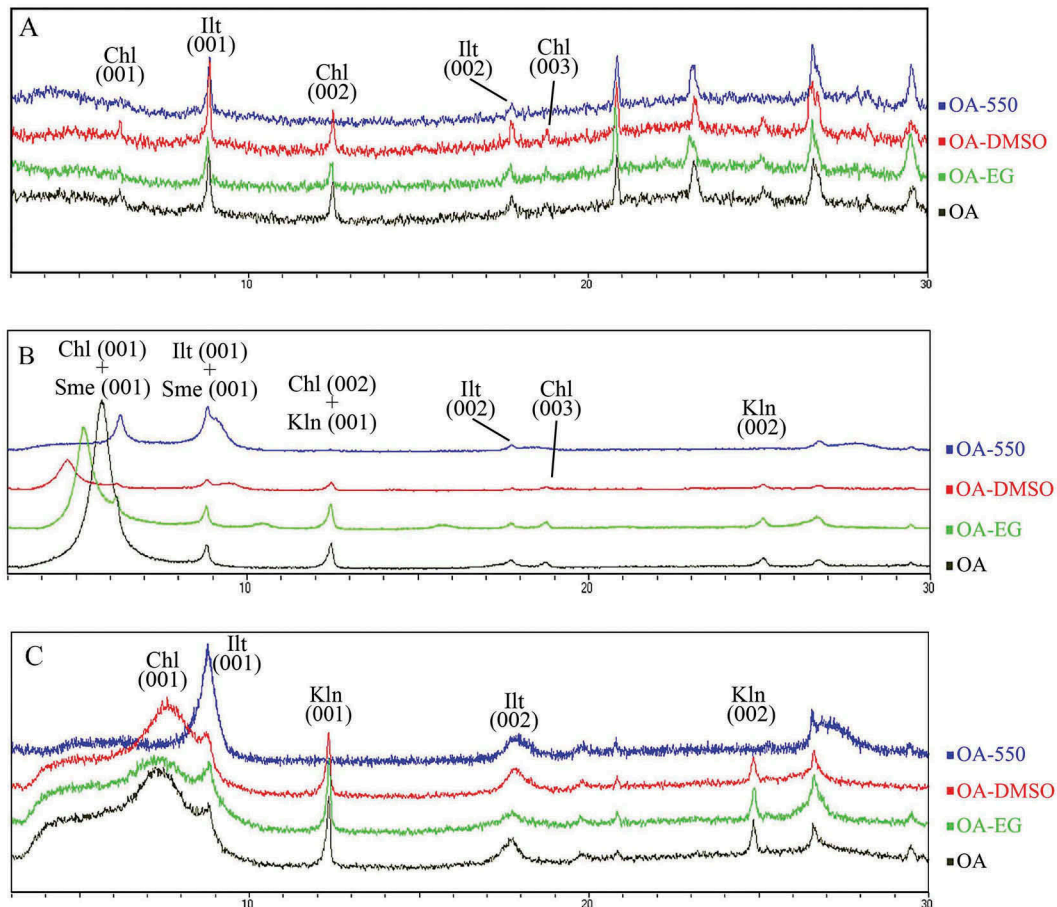


**Figure 3.** XRD patterns of clay fraction: OA: oriented aggregates; OA-EG: oriented aggregates treated with ethylene glycol, OA-DMSO: oriented aggregates treated with dimethyl-sulfoxide, OA-550: oriented aggregates heated at 550 °C; A) beige stone, patterns showing illite and chlorite; B) green-gray stone, peaks showing illite, chlorite and smectite; C) dark-gray stone, the patterns indicating kaolinite and alternating peaks of illite and chlorite.

**Table 3.** XRF results, chemical composition (major elements) of the three types of stone. LLD: low level detection.

Sample	SiO <sub>2</sub> (%)	Al <sub>2</sub> O <sub>3</sub> (%)	Fe <sub>2</sub> O <sub>3</sub> (%)	MnO (%)	MgO (%)	CaO (%)	Na <sub>2</sub> O (%)	K <sub>2</sub> O (%)	TiO <sub>2</sub> (%)	P <sub>2</sub> O <sub>5</sub> (%)	Zr (ppm)	LOI (%)	Total
B1	0.02	<LLD	0.01	<LLD	0.15	56.43	0.02	<LLD	<LLD	0.01	<LLD	42.97	<b>99.61</b>
B2	0.01	<LLD	0.01	<LLD	0.11	56.46	0.03	<LLD	<LLD	0.01	<LLD	42.66	<b>99.29</b>
B3	0.08	0.01	0.02	<LLD	40.8	50.66	0.03	0.01	<LLD	0.02	<LLD	13.92	<b>99.54</b>
GG1	12.46	0.65	0.58	0.02	0.52	47.55	0.04	0.11	0.02	0.02	8.7	37.52	<b>99.49</b>
GG2	7.56	0.53	1.03	0.03	0.44	50.03	0.02	0.09	0.01	0.04	3.7	39.65	<b>99.43</b>
DG1	4.06	1.28	0.36	0.01	0.49	51.52	0.03	0.21	0.05	0.03	10.1	41.4	<b>99.44</b>
DG2	5.01	1.54	0.39	<LLD	0.52	50.52	0.05	0.28	0.06	0.04	9	41.42	<b>99.83</b>

The results of the XRF analyses are presented in Table 3. The beige samples have a significant amount of CaO, B1, and B2 have about 56 wt.% and B3 about 50 wt.%. In sample B3, MgO is also present (ca. 5 wt.%), while it is a minor component in samples B1 and B2 (0.15 and 0.11 wt.%, respectively). The other elements are present in trace amounts.

The main constituent of the green-gray stone is CaO (47–50 wt.%) and the SiO<sub>2</sub> content is higher compared to B (7 and 12 wt.%). Fe<sub>2</sub>O<sub>3</sub>, Al<sub>2</sub>O<sub>3</sub>, MgO, and K<sub>2</sub>O were also detected in small amounts (less than 1 wt.%). The results show that the two macroscopically different green-gray stones (one with fine grain size and the other coarse grain) have similar compositions.

The main component of the dark-gray stone is CaO and other elements such as SiO<sub>2</sub>, Al<sub>2</sub>O<sub>3</sub>, MgO, Fe<sub>2</sub>O<sub>3</sub>, and K<sub>2</sub>O were detected in small amounts.

## 3.2 Petrographic study

### 3.2.1 Beige stone

Two different textures were observed in the beige stone. Samples B1 and B2 had a hypidiotopic calcite texture, which indicates recrystallization of this carbonate under pressure (Flügel and Munnecke 2010). The beige stone can be classified as a limestone. The matrix is slightly micritic and some fine dark particles are scattered in the calcite texture. These may be Fe oxides or hydroxides. Some of the pores are filled with secondary calcite (Figures 4A and 4B). FESEM images of sample B1 have a homogenous texture with low porosity.

EDX analysis of the stone showed that the main chemical element in sample B1 is Ca. We analyzed a crystal around one of the pores, which is brighter than the stone matrix. It is composed of Na, Si, Al, K, and Fe, which is related to illite as identified in XRD (Figure 4D a). The detection of Ti may be due to the presence of rutile (TiO<sub>2</sub>), a commonplace mineral in carbonate stones (Ibbeken and Schleyer 2013; Klein and Hurlbut 1999). Coarse crystals of secondary calcite and bright secondary iron compounds are visible around the pores (Figures 4C and 4D).

Photomicrographs of sample B3 include a mosaic texture consisting of well sorted hypidiotopic anisotropic calcite and xenotopic dolomite minerals in the micrite. Rhombohedral crystals with distinct cleavage stained with alizarine red S prove the presence of dolomite in this sample. Another sign of dolomitization is the brighter border of rhombohedral crystals (Figures 4E and 4F). Elemental analysis of some of the crystals around the pores shows Ca and Mg as major elements

that prove the presence of dolomite. Al and Si were also detected which are related to the presence of clay minerals, particularly chlorite as identified in XRD (Figures 4G and 4H).

### 3.2.2 Dark-gray stone

A petrographic examination of the dark-gray stone (DG1 and DG2) indicated a typical biomicrite stone with crosscutting veins (Figure 5A) and signs of high pressure during several periods of diagenesis which transformed sediments into rocks. Due to the presence of a large amount of clay, the stone suffered high diagenesis pressure (Bausch 1968), which caused some veins and fractures. These veins and fractures are filled with secondary calcite and iron-bearing compounds and their dark appearance is due to the probable presence of organic matter (Figures 5A and 5B) (Flügel and Munnecke 2010). Dark-gray stone can be classified as a limestone in which microfossils such as foraminifera, Hedbergella and Globigerina appear (Figure 5B).

SEM images (Figures 5C and 5D) highlight the fine texture and the morphology of microfossils. The crosscutting veins and fractures have a different texture and some fractures are almost empty, due to fenestral porosity (Lucia 2007). EDX analysis along one of these veins showed that Ca was the main element together with Mg, Si, and Al, which reveal the presence of clay minerals such as chlorite. A second analysis showed the presence of K, which is related to illite as identified in XRD analysis.

### 3.2.3 Green-gray stone

Optical microscopy observation of the green-gray stone revealed a texture with different grain sizes (coarse in GG1 and fine in GG2), made up of calcium carbonate crystals and small amounts of quartz, opal, and clay minerals filled by micro-sparite cement (Figure 5E). This stone can be classified as limestone with small amounts of fossils and interclast. Although this stone has good sorting, GG1 has many pores that may be due to the presence of clay that could have been removed during the preparation of the thin section. Brown-violet particles in polarized light illumination were identified as opal (Figure 5F).

SEM observations (Figures 5G and 5H) showed that mineral particles are scattered in the microstructure of the stone. EDX analysis of the bright gray phase revealed the presence of calcium carbonate, while the darker gray phase were quartz grains. Mg, Al, Fe, and K elements found at the edges of vugs were identified as clay minerals.

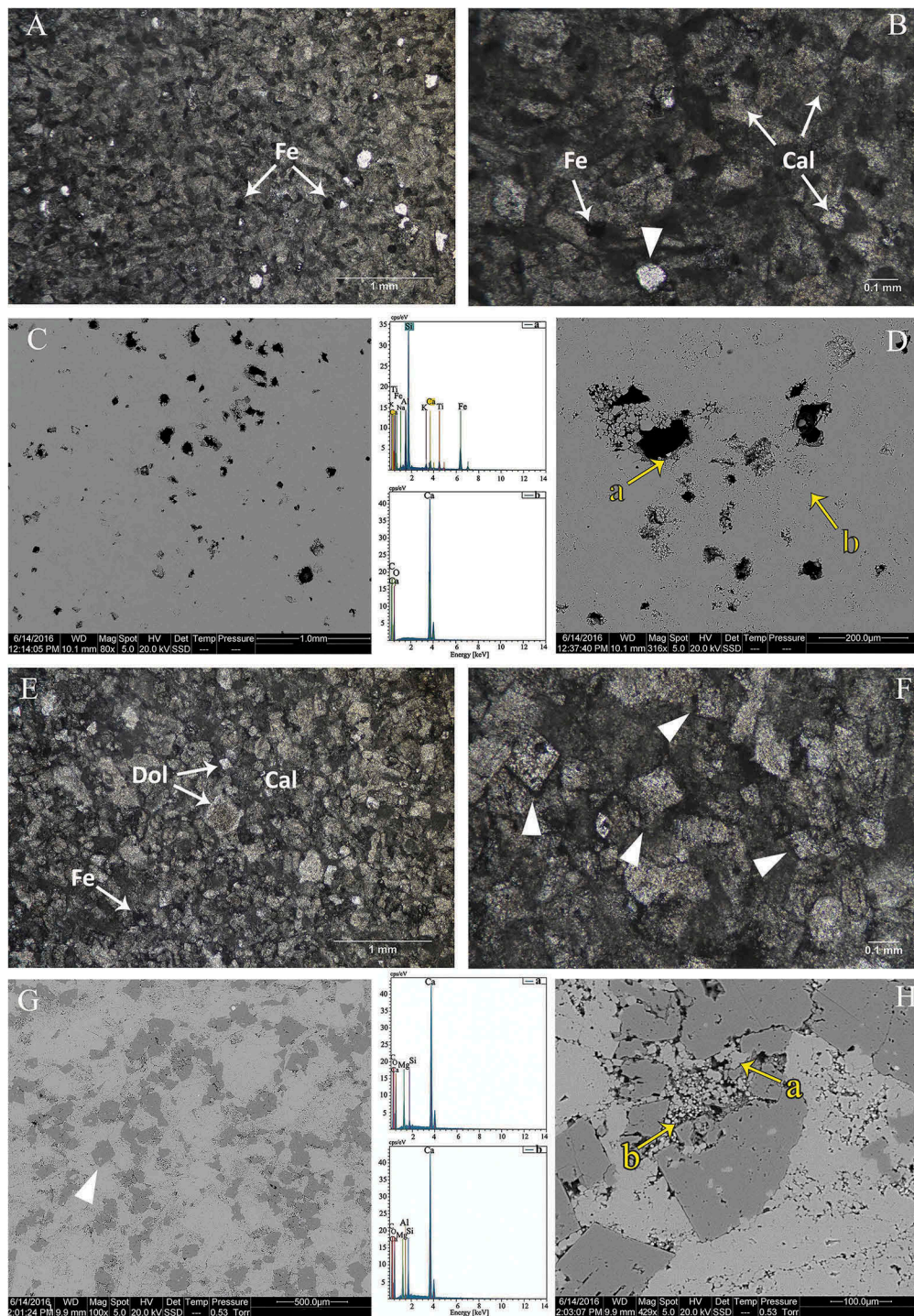


**Figure 4.** OM images of B1 thin section, showing its hypidiotopic calcite texture, and some dark particles associated with a secondary iron component; B) Photomicrographs of B2 indicate the same texture including Cal crystals, secondary Fe Particles and the pores filled with secondary calcite; C) SE image of B1, gray context is  $\text{CaCO}_3$  and the dark spots show the porosity distribution; D) SE image of B1, EDX from point a indicates Ca, Si and Fe as the major chemical elements, EDX from point b shows  $\text{CaCO}_3$  as a main phase; E) Photomicrographs of B3 show hypidiotopic anisotropic calcite and xenotopic dolomite minerals as well as dolomitization, calcite minerals, some dark particles related to the Fe component; F) polarized photomicrographs of B3, distinct dolomite cleavage surfaces are specified by triangles; G) SE image of B3, gray context is  $\text{CaCO}_3$  and the darker points show the dolomite crystals, one of which is indicated by a triangle; H) SE image of B3, EDX from point a indicates Ca, Mg, Si as major elements and EDX from point b indicates Ca, Al, Mg, Si.

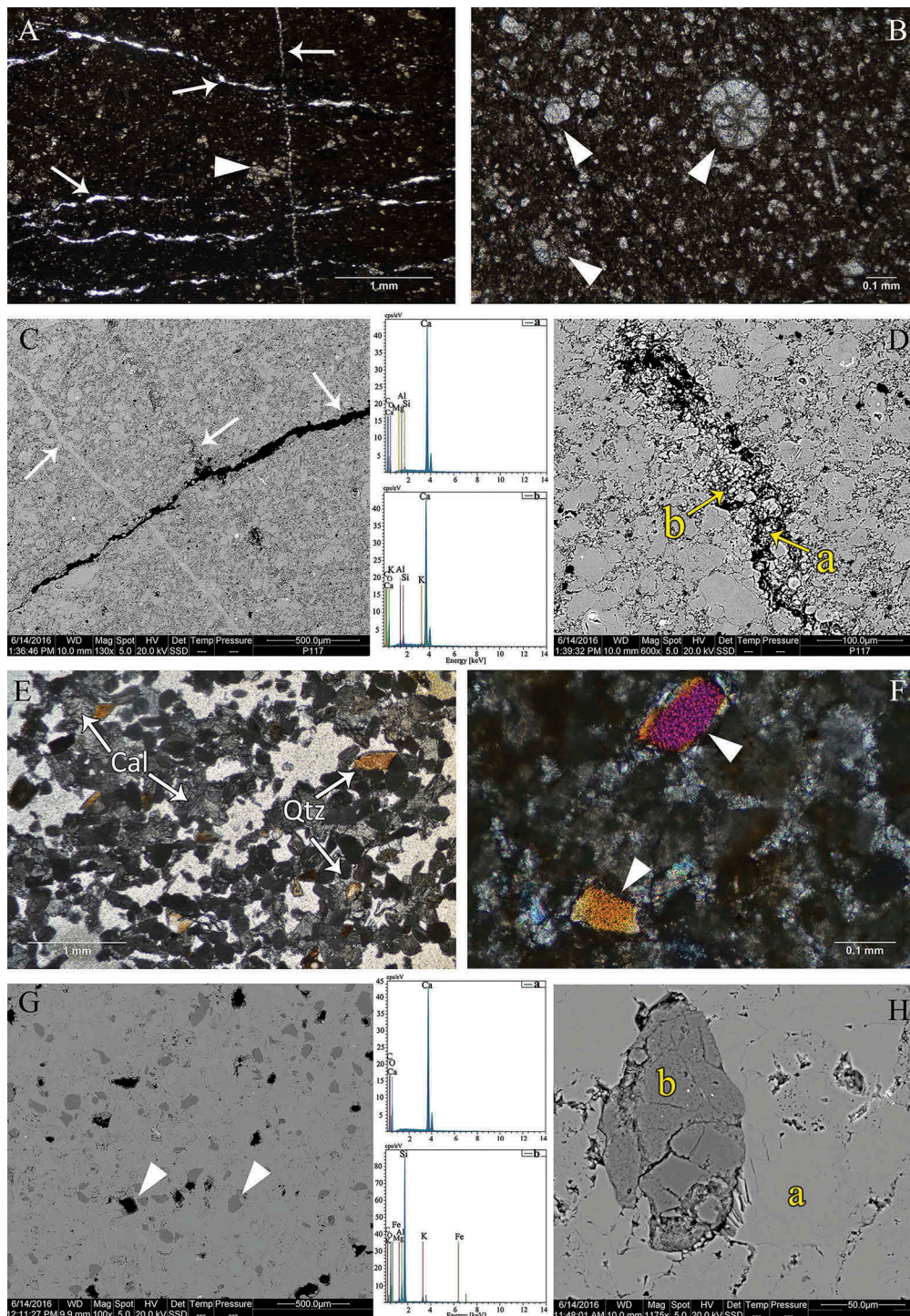


**Figure 5.** A) OM images of DG1 showing biomicrite stone with crosscutting veins, which are indicated by arrows; B) Polarized Photomicrographs of DG2. Some microfossils such as foraminifera and Hedbergella are indicated by triangle shapes; C) SE image of DG1, arrow shapes show empty fracture (fenestral porosity) and vein filled with CaCO<sub>3</sub>; D) SE image of DG1, EDX from point a indicates Ca, Mg, Al, Si as major elements and EDX from point b indicates the presence of Ca, Al, K, Si; E) photomicrographs of GG1 (larger grain size) indicate several different particles such as calcite, quartz and opal; F) Polarized photomicrographs of GG2 show smaller crystals, including calcite and opal (in violet color); G) SE image of GG2, triangle shapes show a vug (in black) and a quartz particle (in dark-grey); H) SE image of GG2, EDX from point a indicates Ca, C, O as the major elements and EDX from point b indicates Si, Al, K, Mg, Fe.

### 3.3 Stone decay

#### 3.3.1 Microscopic observations

**Beige stone.** The videomicroscope images (Figures 6A, 6B, and 6C) show that almost all the beige stone blocks have suffered scaling and pitting damage, apparently due to the activity of microorganisms. There are remains of lichens in some pits, while others have no biological remains at all. The morphology of the black spots inside the surface pores suggests that they are micro-colonies of fungi. Some white minerals similar to efflorescences were observed beside the lichen bodies. These minerals may be some kind of by-product of lichen activity (González-Muñoz et al. 2010; Rodríguez-Navarro et al. 2007) or salt efflorescence. In Figure 6, we can see that the microorganisms have grown in both epilithic and endolithic form. This was confirmed by the presence of fungi hyphae and thalli inside the pores on the surface of the stone.

**Dark-gray stone.** Some of the veins and cracks in the structure of the dark-gray stones are filled with secondary calcite (Figures 6D and 6E). Some of these microfractures run along the sedimentation plane of the stone while others are formed in different directions. This illustrates how the microfissures developed during diagenesis of the stone (Figure 6F).

**Green-gray stone.** Our observations of the green-gray stone revealed micro-cracks and intergranular separation in the stone. Some calcite and quartz particles are visible at higher magnifications (Figure 6I). There is also evidence of biological remains such as fungi and lichen, visible on the surface of some stone blocks (Figure 6H); the fine black grains suggest the concentration of fungi beside the lichen organism (Cámara et al. 2015). We also observed some white materials around the lichens. These may be related to the

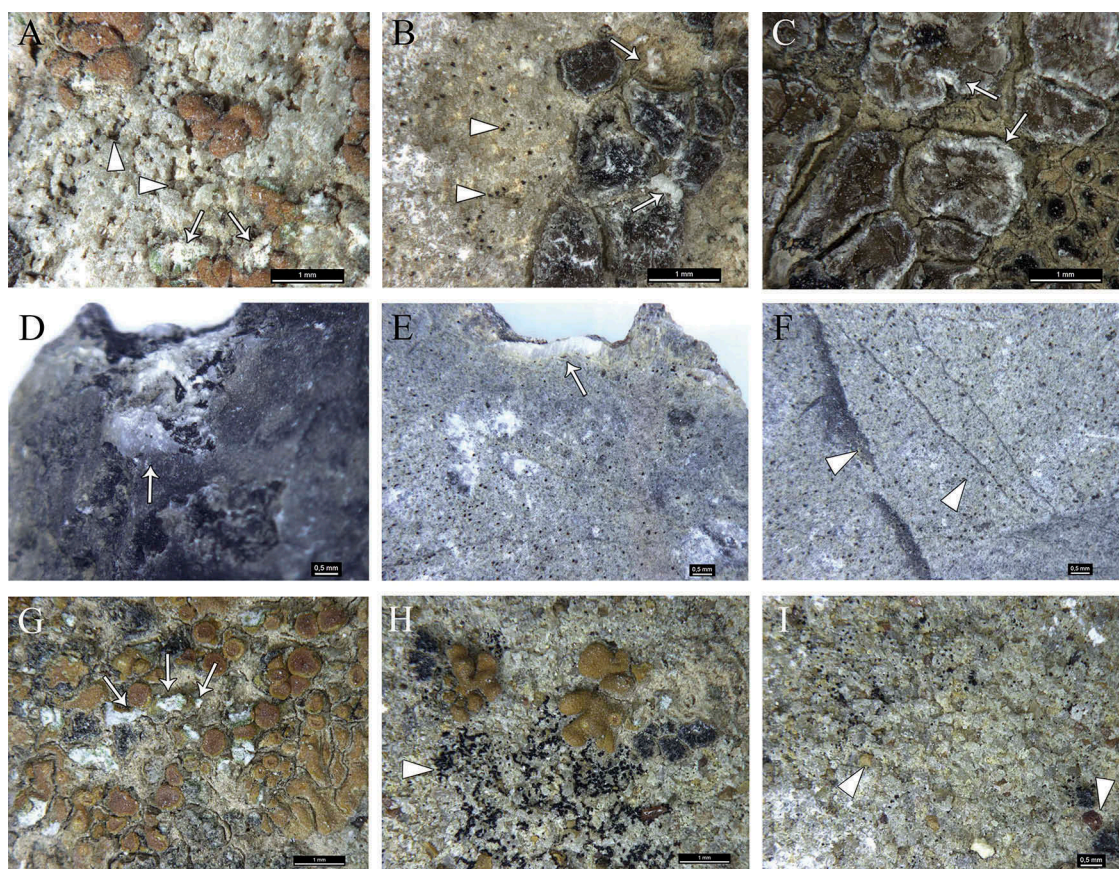


**Figure 6.** A) B.C3, biological pitting decay caused by endolithic thalli shown by triangle shapes and some biomineralization or salt efflorescence visible beside the lichen body shown by arrows; B) B.C3 sample, black spots on the stone surface indicate colony of fungi and arrows show biomineralization; C) B.R1, lichenized surface of stone. Arrows indicate biomineralization or salt efflorescence; D) DG.S1, vein filled with secondary calcite is indicated by the arrow; E) DG.P1 sample, crystals of secondary calcite can be seen at the place where fragments have become detached; F) DG.P1, black spots indicate the micro-colony of fungi, the darker veins in different direction are indicated; G) GG.P2, lichenized surface of stone, arrows indicate the biomineralization; H) GG.P2, the triangle points to a fungi colony; I) GG.P1, the sugaring decay phenomenon is obvious on the surface of the stone and the separation of quartz and opal particles is indicated with triangles.

biomineralization activities of these microorganisms or to salt efflorescence (Figures 6G, 6H, and 6I).

### 3.3.2 FESEM observation and EDX microanalysis

**Beige stone.** A detailed observation of sample B.C1 under FESEM revealed that some of the pores are full of calcium carbonate, while others remain empty (Figure 7A). High magnification of sample B.C2 reveals serious deterioration including hyphae of fungi and holes caused by them (Figure 7B). The main deterioration factor in sample B.C2, which was thought to have been damaged by temperature fluctuation (micro-cracks at grain boundaries) (Luque et al. 2011; Sassoni et al. 2017) was in fact biological activity. The dissolution of calcite crystals was only detected in sample B.C3 (Figure 7C). These samples suffered microorganism attack, which caused serration in the calcite crystals due to dissolution.

Low-magnification images of B.R2 (winged Fig.) and BT1 (Toll-e Takht) show that the surface of these samples is covered by a patina. In the B.R2 sample, some parts of the layer are removed and  $\Lambda$ -shaped serrations created by the dissolution of calcite are evident (Figure 7D). The

patina layer of B.T1 is more regular and compact in comparison with the layer in B.R2. In Figure 7E, EDX analysis indicates the presence of Ca, P, and Si; P may be related to calcium phosphate such as apatite or hydroxylapatite, which is regarded as a biofilm in similar cases (Decho 2000; González-Muñoz et al. 2010). In Figure 7F, some hexagonal plates are visible beside the broken crystal above the patina layer of B.R3. EDX analysis of these plates showed the presence of Ca and S suggesting the crystallization of gypsum.

**Dark-gray stone.** No evidence of bioactivity was found in sample DG.P1 (Figure 8A). A row of large secondary calcite crystals was located between the fine crystals of stone. Some micro-cracks and detachment were detected in DG.S1 next to some clay minerals among the calcite crystals at higher magnification (Figure 8B). EDX analysis detected Si, Al, Mg, K, and Fe elements indicating the presence of clay minerals (CL, Figure 8B).

**Green-gray stone.** In Figures 8C–E, grain separation can be seen in GG.P1. Some channels have been formed

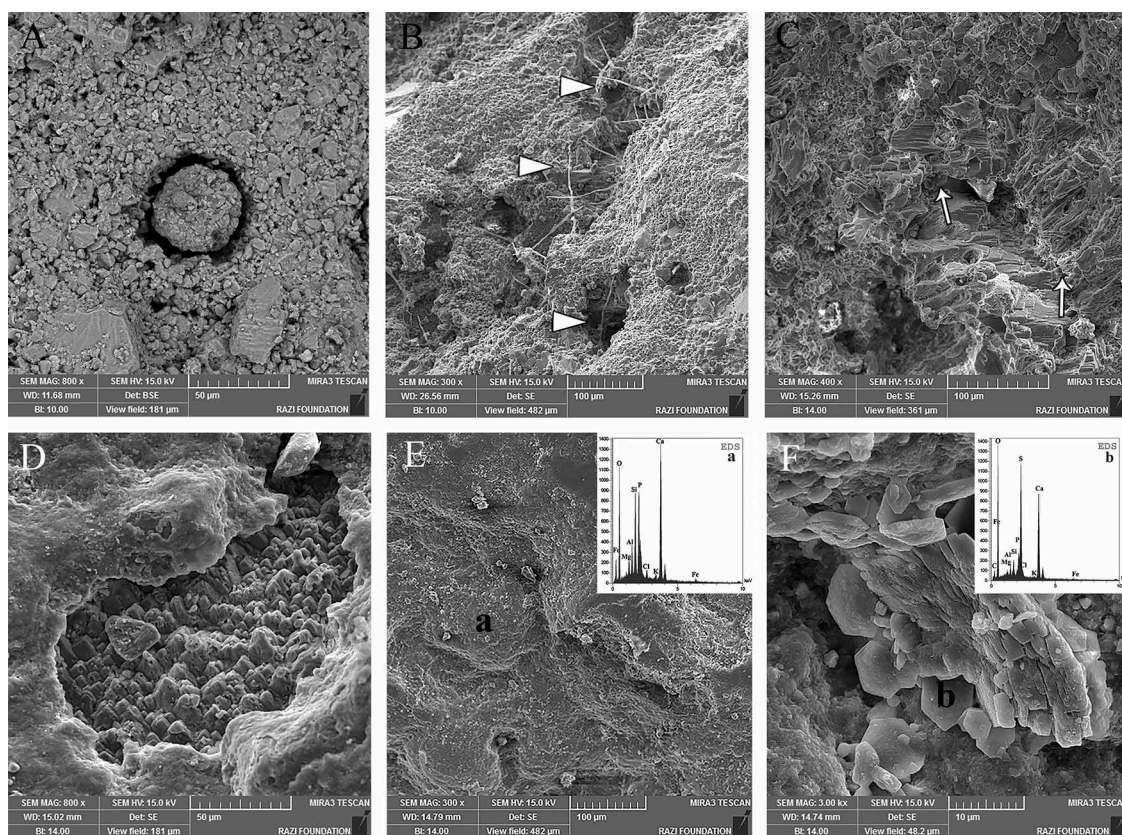


**Figure 7.** A) B.C1, bio-pitting filled by biomineralization; B) B.C2, triangles indicate lichen hyphae; C) B.C3, calcite dissolution causing appearance of channels and serration due to dissolution; D) B.R2, amorphous patina layer and serrations due to dissolution of calcite beneath it; E) B.T1, compact amorphous patina layer, inset: EDX analysis of point a indicating calcium phosphate composition and soil elements; F) B.R3, high magnification of the particle indicated by a rectangle in the patina in image B above, inset: EDX analysis showing that the hexagonal plates may be calcium sulfate.

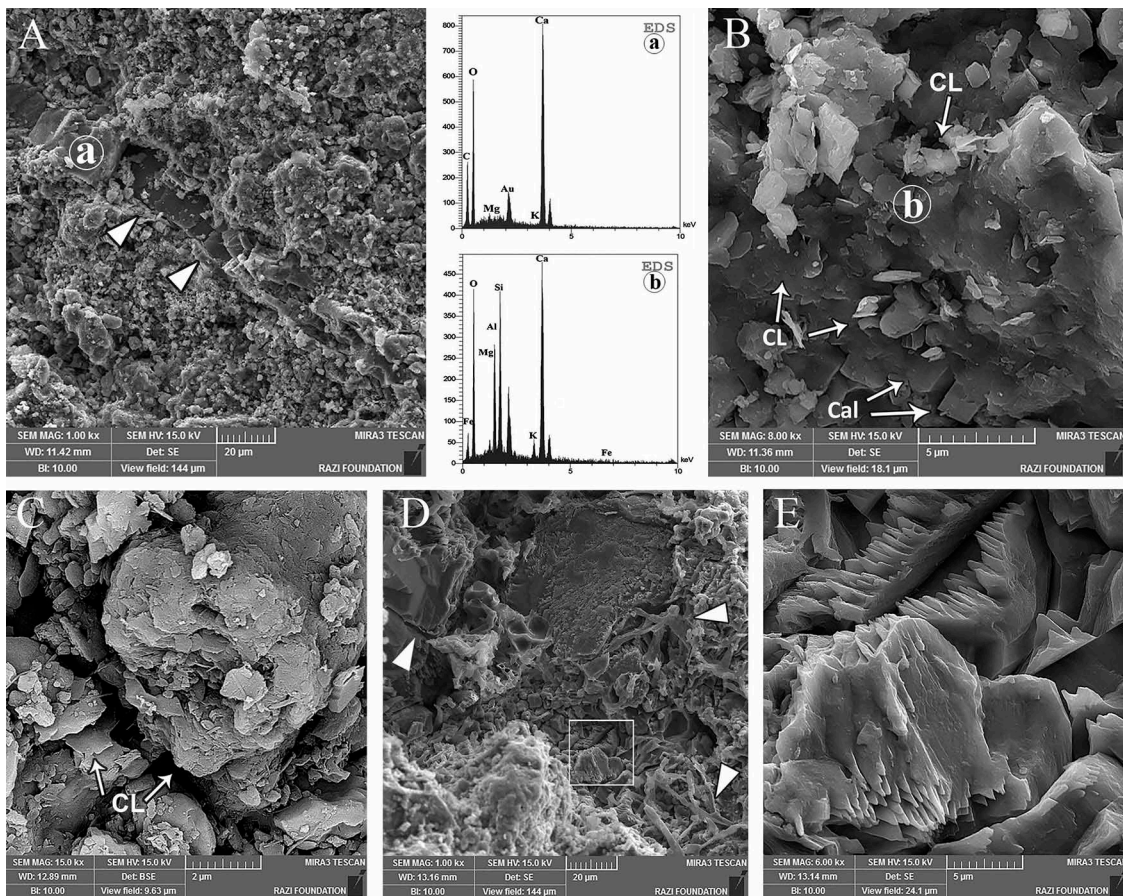


**Figure 8.** A) DG.P1, calcium carbonate texture including a row of coarse crystals (point a). EDX analysis of these crystals reveals calcium carbonate as a major phase; B) DG.S1, distinct calcite crystals (Cal) and flat clay minerals (CL) are visible. EDX of point b proves the presence of clay minerals; C) GG.P1, some evidence of decay phenomena can be observed, such as dissolution channels, detached particles and clay detachment between clay mineral plates; D) GG.P2, triangles indicate hyphae remnants and micro-cracks, E) square indicates high magnification of the crystals, the serrations of the calcite crystals proved the dissolution phenomenon.

by dissolution especially at the contact edge between quartz grains, calcite rehydration and clay minerals (Figure 8C). In sample GG.P2, we detected some remnant hyphae from lichen bodies and micro-cracks. We also observed the presence of some calcite crystals with dissolution serrations. This indicates that this stone has been affected by both dissolution and re-hydration phenomena (Figures 8D and 8E).

### 3.4 Salt and patina analysis

We used XRD to analyze some powdery materials found under the scales (Figure 2 green squares). The results showed that these scales include calcite (the main phase), dolomite, and quartz. No compounds related to soluble salts were found. Moreover, after analyzing the patina layer on the beige stones, we could find no evidence of phases such as oxalates (the usual patina phase in the light-reddish color) or apatite. This is probably due to the small amount of thin patina

layer on the stone surface, which makes it difficult for XRD to detect such small amounts of mineral phases in the compound (Bjelland, Linda, and Thorseth 2002). EDX analysis of the layer found that the patina was composed of calcium carbonate and calcium phosphate acting as a biofilm.

## 4. Discussion

The petrological results indicate that the beige stone has two different compositions: an almost pure sparitic limestone and a dolostone. This means that the stones that had been initially classified as beige stone, purely on the basis of their color, are in fact two different stones with different compositions. The dark-gray is argillaceous limestone with cross cracks and micro-fractures with small amounts of quartz and non-swelling clay minerals (less than 5 wt.%). Finally, the green-gray stone is a sandy limestone with both fine and coarse grains, a quartz content of less than 13% and

the presence of clay minerals such as illite, chlorite, and smectite.

These stones are different from a microstructural point of view and have different deterioration patterns. The beige stone is uniformly composed of calcite and dolomite with a compact, homogenous texture, while the dark-gray stone, despite its low porosity and compact texture, has inherent weakness in its texture due to the presence of defects in the form of large veins filled by secondary calcite with a fine micritic texture. These veins influence the physical-mechanical properties (hardness, strength, breakage) of carbonate stone and may reduce its durability and weathering resistance (Flügel and Munnecke 2010). This is presumably what caused the layered separations in the stone blocks over centuries of weathering. Another possible internal defect in these stones is the presence of clay minerals such as illite and chlorite, whose volume may increase when they come into contact with water through osmotic swelling (Rodríguez-Navarro et al. 1998), thus affecting the shear stress. Moreover, clay and quartz grains have differential hygric stress, which results initially in the detachment of the edges, leading to more serious, large detachments in the long term (Berthonneau et al. 2014; Doehne et al. 2005).

In the green-gray stone, the presence of different phases such as quartz and clay minerals (smectite, illite,

and chlorite) in addition to calcite, causes different decay patterns such as “sanding”. Micro-cracks caused by clay shrinkage indicate differential hygric stress in the clay minerals (Jiménez-González, Rodríguez-Navarro, and Scherer 2008) with respect to the other constituents of the stone texture. In addition, the clay mineral content, and smectite in particular, had a direct influence on its sorption capacity and mechanical characteristics with respect to water content, which in turn govern the level of strength loss (Cherblanc et al. 2016). According to the meteorological data (Figure 9), the average changes of relative humidity (almost between 40% to 80%) during winter and the rainfall (at its highest level) at the same time can lead to swelling of clay minerals of the stones, particularly green-gray.

Moreover, the variety of mineral particles in different colors of green-gray can lead to stress due to temperature fluctuation and the influence of humidity over time (Figure 9). Thermal stress causes shear stress in grain boundaries and the development of cracks that gradually lead to scaling (Doehne Eric and Price 2010), as observed in the field. In addition, daily variation of temperature (almost 25°C in average) beside daily variation of RH (almost 37% in average) and 272 sunny average days throughout the entire year, can cause the continual wetting-drying cycles on the stone surfaces (Table 4).

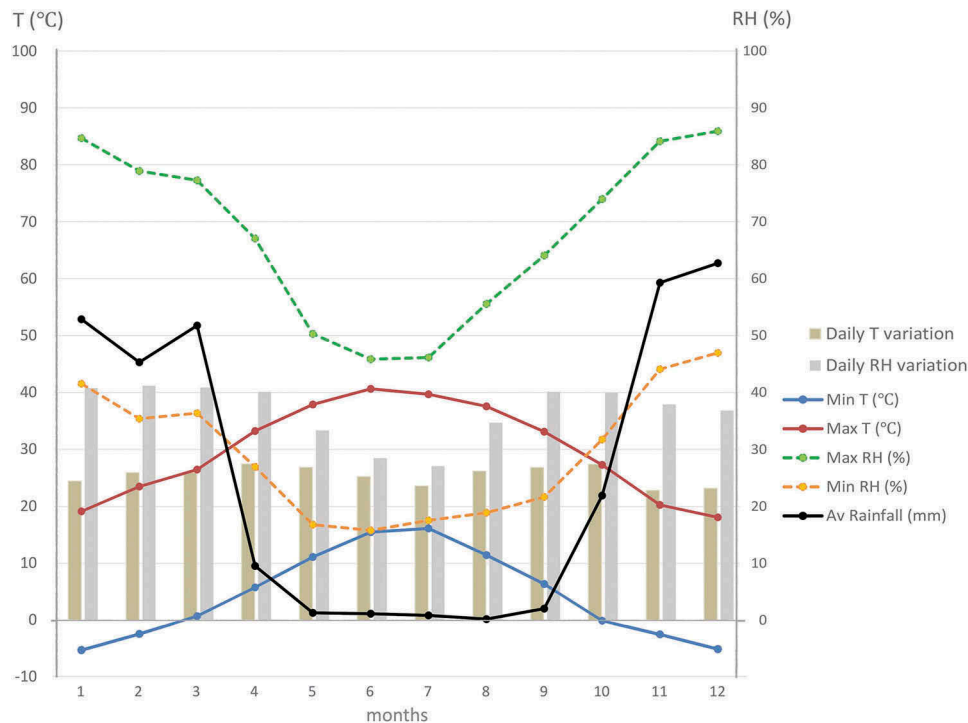


**Figure 9.** Monthly variation of meteorological data of Pasargadae region from 1995-2015 (Iran Meteorological Organization, <http://www.chaharmahalmehmet.ir>).

**Table 4.** Meteorological data of the climate in Pasargadae region from 1995–2015 (Iran Meteorological Organization, <http://www.chaharmahalmehmet.ir>).

	Wind speed Km/h	Daily variation of TEMP °C	Daily variation of RH %	Sunny average days	Freezing average days	Rainy average days
Average	11.66	25.48	36.77	272	55	38

According to the analysis of meteorological data (Figure 9), freeze-thaw cycles take place during three first months as well as two last months of a year. It is clear that freezing occurs when water within the stone actually freezes (McGreevy and Whalley 1982), and during these months the average of minimum temperature is below zero and rainfall is at its highest level. However, the minimum temperature is not less than  $-6^{\circ}\text{C}$  and the average of rainfall is not more than 65 mm over the last 20 years, which does not present a high rate of freezing. It is well known, the stronger damages occur at lower temperature (up to  $-20^{\circ}\text{C}$ ); such as the cracks, the decrease of the elasticity modulus and flexural strength (Grassegger 1999). According to the microscopic observation and meteorological data, freezing cycles happened in Pasargadae stones are not as intense as we initially supposed. Hence, the freezing phenomenon is not a problematic decay factor by itself. However, it should also be borne in mind that low level of freezing beside the other decay factors can influence the rate of damage process.

Field and microscopic observations on the beige stone indicate that biodeterioration such as pitting and chemical deterioration (e.g., dissolution) are the main decay problems affecting the beige stone. Lichens have more serious effects on this stone than on the other types. This may be due to various factors such as its composition, texture, porosity and the roughness of the surface (Miller et al. 2012). In the dark-gray stone lichens were only observed on the parts of the stone where polyester and epoxy (organic materials) were used for restoration purposes (e.g., to join broken pieces), because organic materials offer a good substrate for microorganisms to grow (Ariño and Sáiz-Jiménez 1996; Cappitelli and Sorlini 2008). The green-gray stones resist lichen attack better than the beige stones and have an epilithic-type biocolonization pattern.

Hyphae penetration of the fungi is responsible for the formation of channels and pores in Pasargadae stones. The fact that organic matter such as hyphae fills the pores and leads to a drop in water conductivity (Concha-Lozano et al. 2012a) might have negative effects on stones with low porosity such as the beige stone. This is because the fluctuations in humidity at the Pasargadae site could cause the hyphae to expand

and contract, so increasing the pressure on the pore walls causing micro-cracks to develop in the structure (Ascaso et al. 2002). These expansion and contraction cycles could therefore lead to mechanical decay and scaling in the beige stone.

Given that lichen activity usually results in the deposition of calcium carbonate, calcium oxalate, gypsum, and apatite (González-Muñoz et al. 2010; Mohammadi 2007; Warscheid and Braams 2000), the presence of phosphorous in sample BT1 could be a product of lichen activity, as is the gypsum detected in the patina of Toll-e Takht stone block (BT1), which was formed by the secretion of inorganic sulfuric acid from fungi and its reaction with the calcite matrix of the stone (Scheerer, Ortega-Morales, and Gaylarde 2009). The presence of by-products of lichen activity and fungi hyphae that put pressure on the pore walls should be considered as physical-mechanical decay in Pasargadae stones. By contrast, it has been shown that endolithic organic matter can waterproof the stone (Concha-Lozano et al. 2012a) and that physical-mechanical biodeterioration is slower than the physicochemical decay process (Carter and Viles 2005). It seems likely that hyphae expansion is not as effective as we initially supposed in the decay mechanisms of Pasargadae stones, and we should also consider the physicochemical decay and the morphology of the biofilm.

On the basis of the observations and the analyses conducted on the beige stone blocks, the layer formed on the external part of the stone surface is a regular patina produced by biological activity (Doherty et al. 2007; Hernanz, Gavira-Vallejo, and Ruiz-López 2007; Vazquez-Calvo et al. 2007). SEM-EDX analyses of the patina layer showed the presence of Ca, P, Si, Cl, Fe as well as Ca, S, P elements, which can be attributed to calcium phosphate (e.g., apatite  $[\text{Ca}_5(\text{PO}_4)_3(\text{F},\text{Cl},\text{OH})]$ ) and gypsum ( $\text{CaSO}_4 \cdot 2\text{H}_2\text{O}$ ). There are different opinions about the advantages and disadvantages of microorganism activities and the patinas (biofilm) covering the stone: some authors assume that certain acids such as oxalic, citric, gluconic, and lactic acid produced by lichen activity react with the stone substrate and reduce the strength of the stone minerals (Adamo and Violante 2000). Results of various studies show that the activities of cyanobacteria increase the solubility of limestone (Crispim and Gaylarde 2005; McNamara et al. 2005) and this is visible in the pits on the surface of the beige stone, which were produced by dissolution, while other authors believe that biofilm acts as a protective layer that can buffer the negative effects

of humidity and temperature, such as acid deposition and thermoclastic damage due to intermittent solar radiation (Wendler and Prasartset 1999; Campos-Suñol, Domínguez-Vidal, and De La Torre-López 2008; Concha-Lozano et al. 2012b; b; Salvadori and Municchia 2016). Some researchers emphasize not removing the biofilm (Maxwell 1992; Webster and May 2006).

In the Pasargadae stones, the patina layer covers the surface like a coating. This layer is formed of apatite or hydroxylapatite, which is less soluble and stronger than calcium carbonate when subject to acidic conditions (Hansen et al. 2003). Although these microorganisms caused chemical decay in the past, this resulted in the formation of a calcium phosphate patina, which has beneficial protective effects on the stone. It seems that all the chemical processes led to the formation of a useful biofilm after erosion, which can act as a protective layer against further environmental decay and could therefore be useful in conservation.

## 5. Conclusions

The main phase of the three types of stone used in Pasargadae World Heritage Site is calcium carbonate, which makes up about 90% of their composition. All stones can be classified as limestone except for the beige-colored dolostone. The damage in the green-gray and dark-gray stones is due to structural defects relating to their chemical-mineralogical characteristics. Moreover, daily variation of temperature and fluctuation of moisture can play the main role in the decay of stone surface as well as the clay swelling of the dark-gray stone and in particular of the smectites in the green-gray stone, a fact that must be taken into account in each conservation and restoration step. The main damage factor in the beige stone was lichen activity, even when the stone texture was very compact and homogenous. This indicates that microorganism invasion does not depend on the quality of the stone texture.

The main decay factors in the majority of Pasargadae stone monuments are therefore biodeterioration, the dissolution of stone constituents, and the swelling of clays. The presence of clays in the stones is a problematic issue which raises complex questions for conservators. In a situation like this, controlling clay swelling must take priority over mineral consolidation. For the first step, strict environmental control is recommended (especially wet and dry cycles), and for the second, a treatment to prevent swelling of the clays should be considered as a way of protecting the stones in case of

relative humidity. It should also be borne in mind that the treatment materials do not provide a suitable substrate for the growth of microorganisms.

Although bioactivity normally has negative effects on the rock, in the case of the beige stone this was counteracted by the subsequent formation of a patina layer with a protective role. This layer was composed of calcium phosphate (apatite or hydroxylapatite), which is less soluble and more resistant than calcium carbonate to acidic conditions. It therefore forms a sacrificial layer against further environmental decay, which is useful in conservation and should not be removed.

## Acknowledgments

We thank Prof. Carlos Rodriguez-Navarro, Prof. Eduardo Sebastián Pardo, Dr. Saturnina Henares, Dr. Lucía Rueda Quero, and Dr. Alejandro Burgos-Cara from Department of Mineralogy and Petrology of the University of Granada, Spain; Dr. Beatriz Cámara-Gallego (Spanish National Center for Biotechnology (CNB, Spain)); Dr. Omid Oudbashi (Art university of Isfahan, Iran), Dr. Hamid Fadaei (Department of Conservation and Restoration, Research Institute of Cultural Heritage and Tourism (RICHT, Tehran, Iran), Farzaneh Gerami, Ali Taghva and Hamidreza Karami (Foundation of Pasargadae World Heritage Site, Iran). We are grateful to Nigel Walkington for proofreading the English version of the manuscript.

## Funding

This work was supported by the Research Group RNM179 of the Junta de Andalucía [RNM179]; Research Project MAT2016-75889-R [MAT2016-75889-R]; Ministry of science, research and technology of Iran [215520]. We would like to thank the Razi Applied Science Foundation (Tehran, Iran) and the Centro de Instrumentación Científica (CIC; University of Granada, Spain) for assistance with SEM-EDX analyses.

## ORCID

Atefeh Shekofteh  <http://orcid.org/0000-0003-0664-8476>  
Eduardo Molina  <http://orcid.org/0000-0002-7259-9249>

## References

- Adamo, P., and P. Violante. 2000. Weathering of rocks and neogenesis of minerals associated with lichen activity. *Applied Clay Science* 16 (5):229–56.
- Ariño, X., and C. Sáiz-Jiménez. 1996. Lichen deterioration of consolidants used in the conservation of stone monuments. *The Lichenologist* 28 (04):391–94.
- Ascaso, C., J. Wierzbos, V. Souza-Egipsy, A. De Los Rí, and J. D. Rodrigues. 2002. In situ evaluation of the biodeteriorating action of microorganisms and the effects of biocides on carbonate rock of the Jeronimos Monastery (Lisbon). *International Biodeterioration & Biodegradation* 49 (1):1–12.

- Ashurst, J., and F. G. Dimes. 1998. *Conservation of building and decorative stone*. Abingdon, UK:Routledge.
- Bausch, W. M. 1968. Clay content and calcite crystal size of limestones. *Sedimentology* 10 (1):71–75.
- Berthonneau, J., O. Grauby, E. Ferrage, J. M. Vallet, P. Bromblet, D. Dessandier, D. Chaudanson, and A. Baronnet. 2014. Impact of swelling clays on the spalling decay of building limestones: Insights from X-ray diffraction profile modeling. *European Journal of Mineralogy* 26 (5):643–56.
- Bjelland, T., S. M. B. O. Linda, and I. H. Thorseth. 2002. The occurrence of biomineralization products in four lichen species growing on sandstone in western Norway. *The Lichenologist* 34 (5):429–40.
- Bruton, G. 1955. Vapour glycolation. *American Mineral* 40:124–26.
- Cámara, B., M. Á. De Buergo, R. Fort, V. Souza-Egipsy, S. Perez-Ortega, A. De Los Rios, and C. Ascaso. 2015. Anthropogenic effect on the lichen colonization in building stones from cultural heritage. *Periodico Di Mineralogia* 84 (3):539–52.
- Campos-Suñol, M. J., A. Domínguez-Vidal, and M. J. De La Torre-López. 2008. Renaissance patinas in Úbeda (Spain): Mineralogic, petrographic and spectroscopic study. *Analytical and Bioanalytical Chemistry* 391 (3):1039–48.
- Cappitelli, F., and C. Sorlini. 2008. Microorganisms attack synthetic polymers in items representing our cultural heritage. *Applied and Environmental Microbiology* 74 (3):564–69.
- Carter, N. E. A., and H. A. Viles. 2005. Bioprotection explored: The story of a little known earth surface process. *Geomorphology* 67 (3):273–81.
- Cherblanc, F., J. Berthonneau, P. Bromblet, and V. Huon. 2016. Influence of water content on the mechanical behaviour of limestone: Role of the clay minerals content. *Rock Mechanics and Rock Engineering* 49 (6):2033–42.
- Concha-Lozano, N., P. Gaudon, J. Pages, G. De Billerbeck, D. Lafon, and O. Eterradossi. 2012a. Protective effect of endolithic fungal hyphae on oolitic limestone buildings. *Journal of Cultural Heritage* 13 (2):120–27.
- Concha-Lozano, N., J. Pages, G. De Billerbeck, P. Gaudon, and D. Lafon. 2012b. Bioprotective role of lichens on oolitic limestone buildings. 12th International congress on the deterioration and conservation of stone, New York. Columbia University.
- Crispim, C. A., and C. C. Gaylarde. 2005. Cyanobacteria and biodeterioration of cultural heritage: A review. *Microbial Ecology* 49 (1):1–9.
- Decho, A. W. 2000. Microbial biofilms in intertidal systems: An overview. *Continental Shelf Research* 20 (10):1257–73.
- Doehne, E., S. Simon, U. Mueller, D. Carson, and A. Ormsbee. 2005. Characterization of carved rhyolite tuff—the hieroglyphic stairway of Copan, Honduras. *Restoration of Buildings and Monuments* 11 (4):247–54.
- Doehne Eric, E., and C. A. Price. 2010. *Stone conservation: An overview of current research*, Los Angeles, CA: Getty Conservation Institute.
- Doherty, B., M. Pamplona, R. Selvaggi, C. Miliani, M. Matteini, A. Sgamellotti, and B. Brunetti. 2007. Efficiency and resistance of the artificial oxalate protection treatment on marble against chemical weathering. *Applied Surface Science* 253 (10):4477–84.
- Fitzner, B. 2004. Documentation and evaluation of stone damage on monuments. Proceedings of the 10th international congress on deterioration and conservation of stone, Stockholm, Sweden, 677–90.
- Flügel, E., and A. Munnecke. 2010. *Microfacies of carbonate rocks: Analysis, interpretation and application*. Berlin: Springer-Verlag. ISBN: 978-3-642-03795-5.
- González García, F., and M. Sánchez Camazano. 1968. Differentiation of kaolinite from chlorite by treatment with dimethylsulphoxide. *Clay Minerals* 7:447–50.
- González-Muñoz, M. T., C. Rodríguez-Navarro, F. Martínez-Ruiz, J. M. Arias, M. L. Merroun, and M. Rodríguez-Gallego. 2010. Bacterial biomineralization: New insights from Myxococcus-induced mineral precipitation. *Geological Society, London, Special Publications* 336 (1):31–50.
- Grassegger, G., 1999. Decay mechanisms of natural building stones on monuments—a review of the latest theories. *Werkstoffe und Werkstoffprüfung im Bauwesen*. IWB, Stuttgart, 54–81.
- Haghighat, Z. 2014. *Application of the Dry Ice Blasting method in lichen removal from the historical stone surface (case study: Pasargadae-UNESCO World Heritage Site)*. Art university of Isfahan, Faculty of Conservation and Restoration, Department of Conservation and Restoration of historical artifacts, Isfahan.
- Hansen, E., E. Doehne, J. Fidler, J. Larson, B. Martin, M. Matteini, C. Rodríguez-Navarro, E. S. Pardo, C. Price, A. De Tagle, and J. M. Teutonico. 2003. A review of selected inorganic consolidants and protective treatments for porous calcareous materials. *Studies in Conservation* 48 (sup1):13–25.
- Hernanz, A., J. M. Gavira-Vallejo, and J. F. Ruiz-López. 2007. Calcium oxalates and prehistoric paintings. The usefulness of these biomaterials. *Journal of Optoelectronics and Advanced Materials* 9 (3):512–21.
- Ibbeken, H., and R. Schleyer. 2013. *Source and sediment: A case study of provenance and mass balance at an active plate margin (Calabria, southern Italy)*. Springer Science & Business Media, Springer-Verlag, Berlin, Heidelberg.
- Jiménez-González, I., C. Rodríguez-Navarro, and G. W. Scherer. 2008. Role of clay minerals in the physicochemical deterioration of sandstone. *Journal of Geophysical Research: Earth Surface* 113 (F2) 1–17.
- Klein, C., and C. S. Hurlbut. 1999. *Manual of mineralogy*, vol. 2. Reverté New York, NY: John Wiley.
- Lucia, F. J. 2007. *Carbonate reservoir characterization: An integrated approach*. Springer Science & Business Media, Springer-Verlag, Berlin, Heidelberg.
- Luque, A., E. Ruiz-Agudo, G. Cultrone, E. Sebastián, and S. Siegesmund. 2011. Direct observation of microcrack development in marble caused by thermal weathering. *Environmental Earth Sciences* 62 (7):1375–86.
- Martín Ramos, J. D. 2004. X Powder, a software package for powder X-ray diffraction analysis. Lgl. Dep. GR 1001/04 [www.xpowder.com](http://www.xpowder.com).
- Maxwell, I., 1992. Stone cleaning: For better or worse? An overview. Proceedings of the international conference: Stone cleaning and the nature, soiling and decay mechanisms of stone, Edinburgh, April 14–16, 3–49.
- McGreevy, J. P., and W. B. Whalley. 1982. The geomorphic significance of rock temperature variations in cold

- environments: A discussion. *Arctic and Alpine Research* 14:157–62.
- McNamara, C. J., T. D. Perry, K. Bearce, G. Hernandez-Duque, and R. Mitchell. 2005. Measurement of limestone biodeterioration using the Ca<sup>2+</sup> binding fluorochrome Rhod-5N. *Journal of Microbiological Methods* 61 (2):245–50.
- Miller, A. Z., M. A. Rogerio-Candelera, A. Dionísio, M. F. Macedo, and C. Sáiz-Jiménez. 2012. Assessing the influence of surface roughness on the epilithic colonisation of limestones by non-contact techniques. *Materiales De Construcción* 62 (307):411–24.
- Mohammadi, P., 2007. Rock inhabiting and deteriorating fungi from carbonate monuments of Persepolis. Ph.D. Thesis: Universität Oldenburg.
- Mohammadi, P., and N. Maghbol-Balasin. 2014. Isolation and molecular identification of deteriorating fungi from Cyrus the Great tomb stones. *Iranian Journal of Microbiology* 6 (5):361.
- Moore, D. M., and R. C. Reynolds. 1989. *X-ray diffraction and the identification and analysis of clay minerals*, vol. 378. Oxford: Oxford university press.
- Moropoulou, A., N. Kouloumbi, G. Haralampopoulos, A. Konstanti, and P. Michailidis. 2003. Criteria and methodology for the evaluation of conservation interventions on treated porous stone susceptible to salt decay. *Progress in Organic Coatings* 48 (2):259–70.
- Price, D. G. 1995. Weathering and weathering processes. *Quarterly Journal of Engineering Geology and Hydrogeology* 28 (3):243–52.
- Rafiee Fanood, M., and F. M. Saradj. 2013. Learning from the past and planning for the future: Conditions and proposals for stone conservation of the mausoleum of cyrus the great in the World Heritage Site of Pasargadae. *International Journal of Architectural Heritage* 7 (4):434–60.
- Rodriguez-Navarro, C., C. Jimenez-Lopez, A. Rodriguez-Navarro, M. T. Gonzalez-Muñoz, and M. Rodriguez-Gallego. 2007. Bacterially mediated mineralization of vaterite. *Geochimica et Cosmochimica Acta* 71 (5):1197–213.
- Rodriguez-Navarro, C., E. Sebastian, E. Doehne, and W. S. Ginell. 1998. The role of sepiolite-palygorskite in the decay of ancient Egyptian limestone sculptures. *Clays and Clay Minerals* 46 (4):414–22.
- Salvadori, O., and A. C. Mucicchia. 2016. The role of fungi and lichens in the bio deterioration of stone monuments. *The Open Conference Proceedings Journal* 7, 39–54 (April 1).
- Sami, A. 1956. *Pasargadae, the oldest imperial capital of Iran*. Mehr-Aieen, Shiraz.
- Sassoni, E., G. Graziani, G. Ridolfi, M. C. Bignozzi, and E. Franzoni. 2017. Thermal behavior of Carrara marble after consolidation by ammonium phosphate, ammonium oxalate and ethyl silicate. *Materials & Design* 120:345–53.
- Scheerer, S., O. Ortega-Morales, and C. Gaylarde. 2009. Microbial deterioration of stone monuments—An updated overview. *Advances in Applied Microbiology* 66:97–139.
- Siegesmund, S., T. Weiss, and A. Vollbrecht. 2002. Natural stone, weathering phenomena, conservation strategies and case studies: Introduction. *Geological Society, London, Special Publications* 205 (1):1–7.
- Stronach, D. 1985. Pasargadae. In *The Cambridge history of Iran, vol. II: The median and Achaemenian periods*, ed. I. Gershevitch, 838–55. Cambridge: Cambridge University Press.
- Tilia, A. B. 1968. A study on the methods of working and restoring stone and on the parts left unfinished in Achaemenian architecture and sculpture. *East and West* 18 (1/2):67–95.
- Vazquez-Calvo, C., M. A. De Buergo, R. Fort, and M. J. Varas. 2007. Characterization of patinas by means of microscopic techniques. *Materials Characterization* 58 (11):1119–32.
- Warscheid, T., and J. Braams. 2000. Biodeterioration of stone: A review. *International Biodeterioration & Biodegradation* 46 (4):343–68.
- Webster, A., and E. May. 2006. Bioremediation of weathered-building stone surfaces. *TRENDS in Biotechnology* 24 (6):255–60.
- Wendler, E., and C. Prasartset. 1999. Lichen growth on old Khmer-style sandstone monuments in Thailand: Damage factor or shelter? Triennial meeting (12th), Lyon, August 29–September 3, 1999: preprints, vol. 2, 750–54. James & James, ICOM-CC, Lyon, France.
- Google Earth. 2016. Accessed November 10, 2016. [https://earth.google.com/web/@30.19500697,53.17305659,1848.33475472a,1989.15979918d,35y,52.78917581h,44.88946415t,0r/data=CksaSRJDCiUweDNmYWU3MGUwNGVkODFjMGY6MHgyNWFiMmY5ZGy5NGNmMWY0GY\\_JxaUlMT5AISH2YidmlUpAKghQYXNhcmdhZBgCIAE](https://earth.google.com/web/@30.19500697,53.17305659,1848.33475472a,1989.15979918d,35y,52.78917581h,44.88946415t,0r/data=CksaSRJDCiUweDNmYWU3MGUwNGVkODFjMGY6MHgyNWFiMmY5ZGy5NGNmMWY0GY_JxaUlMT5AISH2YidmlUpAKghQYXNhcmdhZBgCIAE).
- Chaharmahal and Bakhtiari Meteorological Administration. 2015. Accessed September 25. <http://www.chaharmahalmet.ir/iranarchive.asp>.